

Equivalent-photon method study of differential cross sections for double ionization of helium by relativistic heavy-ion impact

S. Keller, H. J. Lüdde, and R. M. Dreizler

Institut für Theoretische Physik, Universität Frankfurt, Robert-Mayer-Straße 8-10, D-60054 Frankfurt-am-Main, Germany

(Received 20 November 1996)

We have calculated the probability for double ionization of helium by fast heavy-ion impact in the equivalent-photon picture. We find that the *shape* of differential cross sections is significantly affected by the inclusion of the electron-electron interaction in both the initial and the final channel, but is rather insensitive to the projectile charge and impact velocity. [S1050-2947(97)01006-8]

PACS number(s): 34.50.Fa, 25.75.-q, 34.10.+x

I. INTRODUCTION

Important advances in experimental techniques, notably the development of cold target recoil ion momentum spectroscopy [1,2], have recently led to the first kinematically complete study of double ionization of helium by heavy-ion impact [3]. The most important observations reported in [3] are that the momentum transfer between projectile and target system is extremely small, and the shape of the cross section plotted as a function of both outgoing electron longitudinal momenta cannot be explained unless the electron-electron interaction is taken into account. In an independent-particle picture this function should be spherically symmetric, while the experiment unambiguously shows that the two electrons are preferentially emitted with unequal longitudinal momenta.

While a large number of theoretical papers have dealt with determining the ratio of the relevant total single- and double-ionization cross sections (see, e.g., [4] and references therein), no quantum theoretical studies of differential cross sections for the heavy-ion impact double-ionization process exist in the literature. In [3] the experimental data were compared with classical trajectory simulations [5], where simplifying assumptions had to be made about the correlated initial state of the helium atom (which is classically unstable). On the basis of different models for the classical correlated dynamics of the two electrons, and a similarity of the cross section measured as functions of the longitudinal electron momenta with the corresponding Fourier transform of a correlated model helium wave function, the authors suggest that these spectra are particularly sensitive to the electron-electron interaction in the initial state. The intuitive explanation supplied in [3] is based on the Weizsäcker-Williams equivalent photon picture [6–8]. The absorption of quasireal photons generated by the fast highly charged ion in distant collisions happens on an extremely short-time scale (10^{-18} sec), so that the fully differential multiple-ionization cross section supposedly represents a “snapshot” of the initial-state electron distribution. It is the purpose of the present study to test this interpretation by explicit calculations, using four different models for the description of the initial and final states of the helium atom.

II. THEORY

A. Equivalent-photon method

The equivalent-photon approach to the description of relativistic quantum collision problems is described in numerous textbooks and reviews (see, e.g., [9,10]), so only a very brief outline of this method will be given here. The basic idea is to exploit the analogy between the Lorentz transformed Coulomb field of a high velocity projectile as observed in the rest frame of the target, and two “pulses” of on-shell photons characterized by their energy spectra (in atomic units, $c = 137.035\,989\,5$)

$$n_1(b, \omega) = \left(\frac{Z_p}{\pi}\right)^2 \frac{1}{c} \left(\frac{\omega c}{\gamma v^2}\right)^2 K_1^2\left(\frac{\omega b}{\gamma v}\right), \quad (1a)$$

$$n_2(b, \omega) = \left(\frac{Z_p}{\pi}\right)^2 \frac{1}{c} \left(\frac{\omega c}{\gamma v^2}\right)^2 \frac{1}{\gamma^2} K_0^2\left(\frac{\omega b}{\gamma v}\right) \quad (1b)$$

and their polarizations $\epsilon_1 = (1,0,0)$, $\epsilon_2 = (0,0,1)$. Here, the (x,z) plane has been taken as the scattering plane with the beam directed along the z axis and b the impact parameter. Z_p , v , and $\gamma = 1/\sqrt{1-(v/c)^2}$ are the projectile charge, velocity, and Lorentz kinematic parameter, respectively, K_0 and K_1 are modified Bessel functions. This analogy allows the collision problem in question to be described in terms of an equivalent-photon-induced reaction: If the cross section for such a process is denoted by $d\sigma_\gamma(\epsilon, \omega, \chi_{final})$ (where χ_{final} denotes the set of observed final-state quantum numbers), for a given impact parameter the cross section sought is given by integrating over the number spectra of the photon pulses,

$$d\sigma(b, \chi_{final}) = \sum_{i=1}^2 \int_0^\infty \frac{d\omega}{\omega} n_i(b, \omega) d\sigma_\gamma(\epsilon_i, \omega, \chi_{final}), \quad (2)$$

and accordingly for processes involving multiple photons. In Eq. (2), a sum over polarization directions is involved, which is frequently disregarded in the literature because it is irrelevant for the total cross sections usually considered. The use of the photo cross section $d\sigma_\gamma$ (rather than of the corresponding matrix element) in Eq. (2) is a manifestation of the basic assumption that the effects of the various frequency

components of equivalent radiation add incoherently [9]. This also implies that the interference of different reaction mechanisms cannot be discussed within this approach. The assumption just mentioned will be reasonable if the projectile field can be considered as a small perturbation. Indeed the equivalent-photon method can be considered as a technique for estimating the leading terms of the perturbation expansion of the scattering matrix in powers of $Z_p e^2$ by subsequently considering the contributions of processes involving increasing numbers of photons.

Apart from this intrinsic limitation to the perturbative regime, the equivalent-photon approach suffers from a number of technical deficiencies. In particular, it is rigorously valid only in the limit $v \rightarrow c$, and it requires the *ad hoc* introduction of a lower cutoff impact parameter in total cross-section calculations because the equivalent-photon picture is inappropriate if the projectile penetrates the target system. Indeed it turns out that, in the application to be discussed below, the corresponding impact-parameter integral is divergent for $b \rightarrow 0$. However, this is not a serious drawback for the present study because a quantitative comparison with the experimental data of [3] is not intended. Moreover, the fact that the momentum transfer is very small indicates that large impact parameters are most important for the processes in question. Consequently, we will presently discuss only the situation of a single fixed impact parameter ($b=5$ a.u.).

B. Ionization mechanisms

It is generally assumed that the double-ionization process at high impact energies is dominated by two mechanisms which can be discussed in the framework of perturbation theory. The shake-off process is characterized by a single ion-electron interaction leading to ionization. The second electron is subsequently ejected because its initial-state single-particle wave function has nonvanishing overlap with the continuum of the singly charged ion produced in the collision. This is the only first-order process (order $Z_p e^2$) leading to double ionization, hence shake-off is expected to dominate at very high energies. It has been found, however, that even at impact energies of several MeV/amu, the second-order two-step mechanism of subsequent ionizing interactions of the projectile, with both electrons, cannot be neglected [11]. The alternative two-step mechanism in which the projectile ionizes one electron which subsequently undergoes an ionizing collision with the second electron, is of order $Z_p e^4$, rather than $Z_p^2 e^4$, and therefore of minor importance for the case of heavy-ion impact.

The equivalent-photon analog of the shake-off mechanism is the photo double-ionization [or $(\gamma, 2e)$] process. In the dipole approximation, the relevant fully differential cross section is

$$\frac{d^6 \sigma_{(\gamma, 2e)}}{d^3 k_a d^3 k_b} = \frac{(2\pi)^2}{\omega} | \langle k_a k_b | \vec{\epsilon} \cdot \hat{d} | \Psi_0 \rangle |^2, \quad (3)$$

where k_a, k_b are the outgoing electron momenta, $\vec{\epsilon}$ is the incident photon polarization, \hat{d} the dipole operator (that we use in the velocity form), while $|\Psi_0\rangle$ and $|k_a k_b\rangle$ denote the initial and final eigenstates of the helium-atom Hamiltonian, respectively (antisymmetrization is understood).

The two-step process discussed above can be reinterpreted in terms of double ionization by means of two independent photon-induced single-ionization events. Indeed it is usually assumed that this mechanism is composed of two statistically independent single-ionization events (note that the ‘‘snapshot’’ interpretation of the experiment of Ref. [3] refers to this type of process). The corresponding $(2\gamma, 2e)$ cross section reads

$$\frac{d^6 \sigma_{(2\gamma, 2e)}}{d^3 k_a d^3 k_b} = \frac{(2\pi)^2}{\omega_1 \omega_2} | \langle k_a k_b | (\vec{\epsilon}_1 \cdot \hat{d}_1) (\vec{\epsilon}_2 \cdot \hat{d}_2) | \Psi_0 \rangle |^2. \quad (4)$$

Again the dipole approximation has been used. Moreover, in the spirit of the two-step mechanism we assume that each photon is absorbed by one electron (assumed to have either of the experimental binding energies of -0.90261 and -1.992 Hartree), so that by energy conservation both frequency integrations over the pertinent equivalent-photon number spectra collapse.

It is worth noting at this point that for the case of an initial $1s^2$ state, the final continuum states accessed by the $(\gamma, 2e)$ mechanism have (sp) symmetry, while the $(2\gamma, 2e)$ mechanism leads to a (pp) state [12]. Therefore, the interferences between the two types of amplitudes can for the qualitative considerations of the present study be neglected. This is consistent with the basic assumption of the equivalent-photon method discussed above.

C. Choice of wave functions

The $(\gamma, 2e)$ cross section, differential in electron momenta, is now accessible to experiment [13,14]. This has stimulated numerous theoretical studies of this reaction [15–19]. However, it had been realized much earlier that this process is entirely due to the electron-electron interaction [20–22]. While these earlier studies focused on the effect of the electron-electron interaction in the *incident* channel, the more recent results emphasize the importance of *final*-state interactions. This implies that both effects have to be considered in the present context. In this work, we will ultimately be interested in ‘‘partial’’ differential cross sections which have to be determined by numerical integration of the fully differential cross sections [defined by using Eqs. (3) and (4) in Eq. (2) and its two-photon analog, respectively] over parts of the electronic final-state phase space. Thus the use of the sophisticated theories proposed in [15,19] is out of the question. We therefore consider the following three simple models: (i) the description of the initial state by the one-parameter $1s^2$ type wave function $\Psi_{1s^2} = (Z_{\text{eff}}^3/\pi) \exp[-Z_{\text{eff}}(r_a + r_b)]$, where $Z_{\text{eff}} = 27/16$, and of the final state by a product of plane waves; (ii) the initial state as in Eq. (1), but the final state represented by a product of Coulomb scattering waves with incoming spherical wave boundary conditions; and (iii) the final state as in Eq. (1), but the initial state described by the 46-parameter wave function proposed in [20]. This wave function includes (ss) , (pp) , and (dd) angular correlations, and thus accounts for 95.9% of the experimental correlation energy. For these models, analytical results for the $(\gamma, 2e)$ S matrix elements

may be found in the literature [16,21]. The corresponding $(2\gamma,2e)$ amplitudes have been calculated along the same lines [23].

A major weakness of these models is the fact that the wave functions for the initial and final states are not exact, but only approximate eigenfunctions of the helium-atom Hamiltonian. As a consequence, the transition current is not conserved, so that the results are gauge dependent. To be specific, the results obtained using different forms of the dipole operator differ significantly in absolute magnitude. The shapes of the cross-section function are less affected [16]. We will, therefore, in the present study concentrate on analyzing the shapes of the cross-section function obtained, and not present absolute numerical data.

The postcollisional interaction of the electrons can conveniently be modeled by multiplying the photo cross section with the ‘‘correlation factor’’

$$C(\alpha) = \frac{2\pi}{\alpha} \left[\exp\left(\frac{2\pi}{\alpha}\right) - 1 \right]^{-1}, \quad (5)$$

where $\alpha = |\vec{k}_a - \vec{k}_b|$. $C(\alpha)$ corresponds to the squared modulus of the Coulomb continuum wave describing the two-electron subsystem for zero separation of the two electrons. It has been shown in [16,18] that this procedure is quite reasonable for most kinematical situations, and that it is crucial to include the electron-electron final-state interaction, at least in this form, in order to obtain reasonable cross-section shapes. To obtain the ‘‘partial’’ differential cross sections desired, the fully differential cross sections were integrated over the transverse momentum components using adaptive Monte Carlo techniques [24].

III. NUMERICAL RESULTS

In Figs. 1–4 we present numerical data for the double-ionization cross section as a function of the longitudinal momenta of the outgoing electrons obtained from the different models described above. In order to assess the importance of electron-electron interaction in the final state, we have carried out calculations using model (i) without and with the correlation factor, Eq. (5) [in Figs. 1–4, parts (a) and (b)]. Furthermore, comparison of the results of models (i) and (ii) [in Figs. 1–4, parts (b) and (c)] obtained including this factor allows us to estimate the importance of Coulomb three-body effects in the final state. Finally, discrepancies between data obtained from models (i) and (iii) [in Figs. 1–4, parts (b) and (d)] must be due to the different initial states.

There is a certain amount of ‘‘noise’’ in the data, most notably for the case of initial-state angular correlations. This is due to the limitations of the size of the Monte Carlo samples imposed by computing time considerations [the data of Figs. 1–4, part (d) typically required about 100 CPU days on a RISC workstation]. In the present data, this statistical error is of the order of 5%. To facilitate the understanding of the figures, we remind the reader that the top right quadrant of the plots corresponds to forward emission of both electrons, while the top left and bottom right quadrant represent back-to-back emission. Values close to the Cartesian axes of the plots correspond to asymmetric energy sharing of the outgoing electrons, while the diagonals represent symmetric

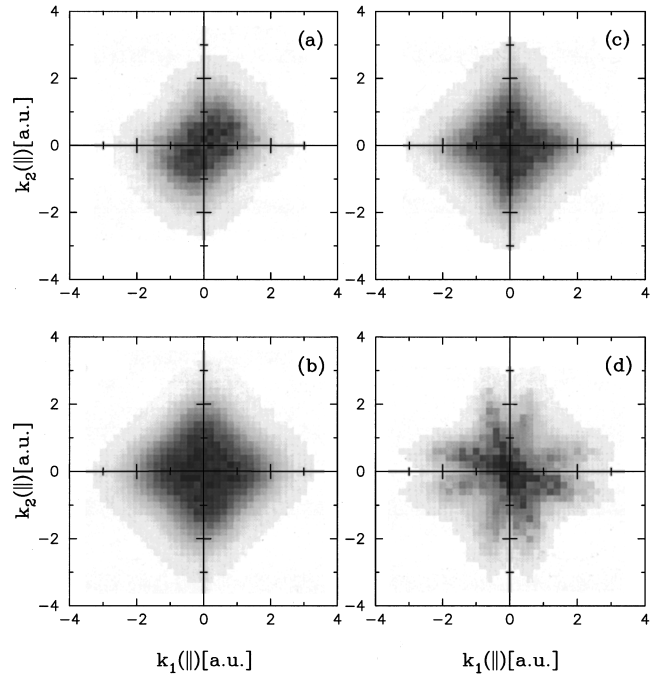


FIG. 1. Cross section for double ionization of helium by heavy-ion impact as a function of the longitudinal momenta of both outgoing electrons (in atomic units). Shake-off process: (a) $(\gamma,2e)$ type cross section, model 1 without correlation factor; (b) $(\gamma,2e)$ type cross section, model 1, correlation factor included; (c) $(\gamma,2e)$ type cross section, model 2, correlation factor included; (d) $(\gamma,2e)$ type cross section, model 3, correlation factor included. Impact energy 3.6 MeV/amu, nuclear charge $Z=28$, and impact parameter 5 a.u.

distributions of kinetic energy. Due to the antisymmetry of the electronic wave functions all results must be symmetric under interchange of the longitudinal momenta with or without change of sign of both momenta. This feature is indeed evident in all figures, demonstrating that the accuracy of the Monte Carlo integration is sufficient for the present purpose.

The impact energy and nuclear charge used for the data of Figs. 1 and 2 correspond to the parameters of the recent experiment [3]. Figures 1 and 2, part (a) exhibit the characteristics of the respective dipole transition matrix elements, Eqs.(3) and (4). For the shake-off process, ejection of both electrons parallel or antiparallel to the beam is favored due to the characteristic structure $|\vec{\epsilon} \cdot \vec{k}_1 S(k_1, k_2) + \vec{\epsilon} \cdot \vec{k}_2 S(k_2, k_1)|^2$ of the cross section in Eq. (3) (with S a function of the magnitudes of the momenta only) which includes a relative minus sign (destructive interference) for back-to-back emission in the case of the second equivalent-photon ‘‘pulse’’ [25]. The two-photon transition cross section takes the form $|(\vec{\epsilon} \cdot \vec{k}_1)(\vec{\epsilon} \cdot \vec{k}_2) S(k_1, k_2)|^2$ [Eq. (4)], which results in a spherical distribution, indicating that the corresponding double-ionization probability is characterized by the total energy transferred to the electrons. The strong decrease of the cross sections for increasing total energy is readily traced to the factor ω^{-2} associated with each photon absorbed. It is worth noting that these calculations already include part of the electron-electron interaction in the initial state due to the choice of the effective charge parameter. Nevertheless, the

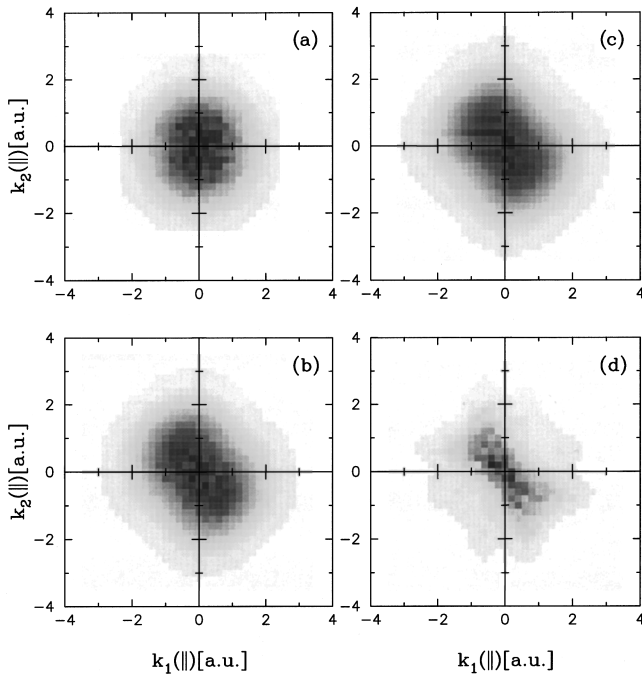


FIG. 2. Cross section for double ionization of helium by heavy-ion impact as a function of the longitudinal momenta of both outgoing electrons (in atomic units). Two-photon process: (a) $(2\gamma, 2e)$ type cross section, model 1 without correlation factor; (b) $(2\gamma, 2e)$ type cross section, model 1, correlation factor included; (c) $(2\gamma, 2e)$ type cross section, model 2, correlation factor included; (d) $(2\gamma, 2e)$ type cross section, model 3, correlation factor included. Impact energy 3.6 MeV/amu, nuclear charge $Z=28$, and impact parameter 5 a.u.

shape of the two-photon cross section is what one would expect from an independent-particle model, which is simply due to the fact that this model is designed to describe two independent photoionization events.

From Figs. 1 and 2, parts (a) and (b) it is evident that for both mechanisms the postcollision interaction of the two electrons significantly suppresses emission of both electrons with the same orientation of longitudinal momentum. This observation is consistent with the fact that the shape of the differential cross section for double ionization near threshold is completely determined by the mutual repulsion of the outgoing electrons, as was already pointed out by Wannier [26]. Indeed the inclusion of the Coulomb interaction between the ejected electrons and the residual ion [Figs. 1(c) and 2(c)] for both types of reaction only marginally affects the shape of the cross-section function.

By contrast, the inclusion of angular correlations in the initial ground-state wave function [Figs. 1(d) and 2(d)] leads to marked changes in the shape of the cross sections. Most notably, for the shake-off reaction the probability for emission of one of the electrons with zero longitudinal momentum is significantly decreased. This finding can be interpreted in terms of the fact that in this case the final state of the “shake-off” electron is not a pure s level, but contains also important contributions of higher angular-momentum states. For the two-photon process, there is no such clear-cut signature. In this case, the main effect of the initial-state angular correlation would seem to be the suppression of ionization into high longitudinal momentum states and an addi-

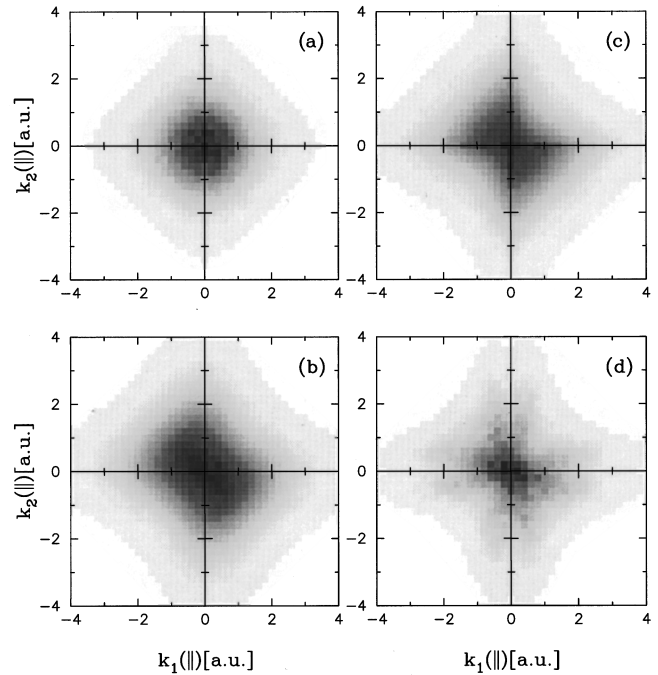


FIG. 3. Cross section for double ionization of helium by heavy-ion impact as function of the longitudinal momenta of both outgoing electrons. Shake-off process, data as in Fig. 1, but for impact energy 2 GeV/amu, nuclear charge $Z=92$, and impact parameter 5 a.u.

tional suppression of emission into the same longitudinal direction.

It is instructive to also consider much higher energies and projectile charges, where the equivalent-photon picture is more appropriate. We have therefore treated the case of double ionization of helium by bare uranium ions at 2 GeV/amu impact energy, corresponding to the maximum values for projectile charge and impact energy currently available at the GSI accelerator facilities. The cross-section functions for this collision system are presented in Figs. 3 and 4. The similarities between these data and those of Figs. 1 and 2 are striking. This can be understood in terms of the fact that, as noted above, emission of the electrons with relatively low (of the order of one atomic unit) kinetic energy, corresponding to the absorption of relatively “soft” equivalent photons, is strongly favored irrespective of the impact energy. Indeed, the only effect of the change of projectile is to modify the spectral weights $n(b, \omega)$, whereas the relevant momentum scales are introduced through the photo cross-section functions which are not changed at all.

A clear discrepancy in the shape of the cross-section function is seen between Figs. 1(a) and 3(a). The interpretation of this result is straightforward: according to Eq. (1), the second photon “pulse” is suppressed in intensity with γ^{-2} relative to the first one, so that the lack of spherical symmetry plays only a marginal role at high energies. The longitudinal momentum distribution of the electrons here follows the one-electron Compton profile. This implies that radial correlations in the initial-state wave function alone do not break the spherical symmetry of the cross-section function in question, as would indeed be expected from symmetry considerations.

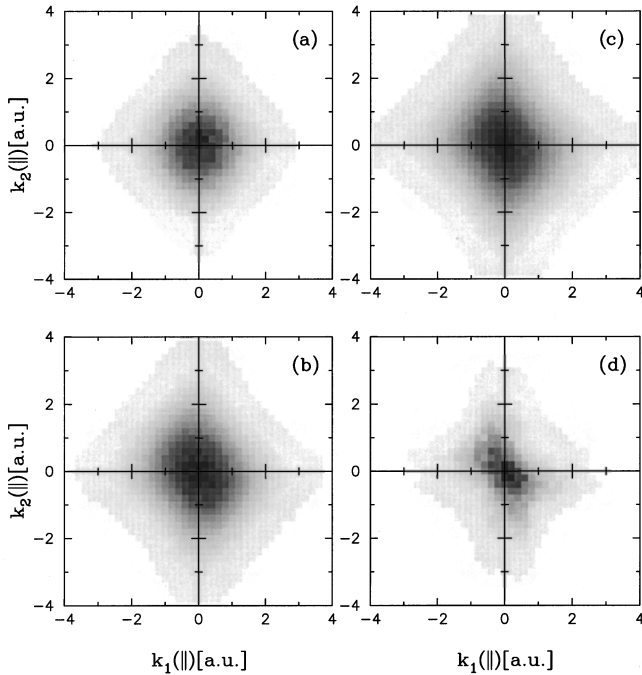


FIG. 4. Cross section for double ionization of helium by heavy-ion impact as function of the longitudinal momenta of both outgoing electrons. Two-photon process, data as in Fig. 2, but for impact energy 2 GeV/amu, nuclear charge $Z=92$, and impact parameter 5 a.u.

IV. CONCLUSIONS

The above numerical results show that the double-ionization cross sections plotted as a function of the longitudinal momenta of the electrons are strongly influenced by the model chosen not only for the ionization mechanism, but also for the treatment of the electron-electron interaction. Our calculations thus confirm the central assertion of [3]. However, concerning the explicit interpretation of the experimental data in terms of the equivalent-photon picture, there are three important caveats.

(1) The validity of the equivalent-photon picture itself is limited to energies of at least a few GeV/amu. The application of the model to the experimental data of [3] can there-

fore only yield qualitative information. Indeed, the fact that the experimental data show a marked shift away from the symmetric point of vanishing longitudinal momenta towards positive longitudinal momenta demonstrates the importance of postcollisional electron-projectile Coulomb interactions, which indicates that the equivalent-photon picture is not really appropriate in this case [25].

(2) For both kinematical situations considered in this paper, the parameter characterizing the perturbation by the projectile, namely, Z_p/v , is of the order of unity. Hence, the interpretation of the experimental data in terms of perturbation theory, which is implicit in the use of the equivalent-photon picture, is in itself questionable. In order to allow for this type of analysis, experiments with fast light ions would be desirable.

(3) Our results demonstrate that the details of the description of both the bound and the continuum states of the interacting electrons have a significant influence on the shapes of the cross sections, irrespective of the impact energy. This is due to the fact that emission with small momentum is favored in any case. Hence, the only simplification which occurs for lighter projectiles and/or very high impact energy is the dominance of single-photon absorption. Still the full complexity of the three-body Coulomb problem will have to be faced.

In order to fully use the potential of the novel experimental techniques presented in [1–3] with regard to spectroscopy of initial-state correlations, it will therefore be necessary to identify more suitable subregions of the final-state phase space. For instance, the explicit form of the Coulomb correlation factor Eq. (5), suggests that the postcollisional interaction between the electrons will essentially provide a common constant overall factor to the differential cross section for all electron pairs with a common value of $\alpha := |\vec{k}_a - \vec{k}_b|$.

ACKNOWLEDGMENTS

It is a pleasure to thank J. Ullrich, R. Moshhammer, and H. Schmidt-Böcking for drawing our attention to this problem and for valuable discussions. S.K. also wishes to thank C. Dal Cappello and B. Joulakian for instructive discussions on related double-ionization problems. We gratefully acknowledge support by the BMBF under Contract No. 06OF739.

-
- [1] J. Ullrich *et al.*, *Comments At. Mol. Phys.* **30**, 70 (1994).
 - [2] R. Moshhammer *et al.*, *Instrum. Methods Phys. Res. B* **108**, 425 (1996).
 - [3] R. Moshhammer, J. Ullrich, H. Kollmus, W. Schmitt, M. Unverzagt, R.E. Olson, C.J. Woods, O. Jagutzki, V. Mergel, H. Schmidt-Böcking, and R. Mann, *Phys. Rev. Lett.* **77**, 1242 (1996).
 - [4] J.H. McGuire, N. Berrah, R.J. Bartlett, J.A.R. Sampson, C.L. Cocke, and A.S. Schlachter, *J. Phys. B* **28**, 913 (1995).
 - [5] R.E. Olson, J. Ullrich, and H. Schmidt-Böcking, *Phys. Rev. A* **39**, 5572 (1989).
 - [6] E. Fermi, *Z. Phys.* **29**, 315 (1924).
 - [7] C.F. Weizsäcker, *Z. Phys.* **88**, 612 (1934).
 - [8] E.J. Williams, *Phys. Rev.* **45**, 729 (1934).
 - [9] J.D. Jackson *Classical Electrodynamics* (Wiley, New York, 1962), Chap. 15.
 - [10] C. Bertulani and G. Baur, *Phys. Rep.* **163**, 299 (1988).
 - [11] J.H. McGuire, *Phys. Rev. Lett.* **49**, 1153 (1982).
 - [12] A.L. Ford and J.F. Reading, *Nucl. Instrum. Methods Phys. Res. B* **10/11**, 12 (1985).
 - [13] O. Schwarzkopf, B. Krässig, J. Elmiger, and V. Schmidt, *Phys. Rev. Lett.* **70**, 3008 (1993).
 - [14] P. Lablanquie, J. Mazeau, L. Andric, P. Selles, and A. Huetz, *Phys. Rev. Lett.* **74**, 2192 (1995).
 - [15] F. Maulbetsch and J.S. Briggs, *J. Phys. B* **26**, L647 (1993).
 - [16] F. Maulbetsch and J.S. Briggs, *J. Phys. B* **26**, 1679 (1993).
 - [17] F. Maulbetsch, M. Pont, J.S. Briggs, and R. Shakeshaft, *J. Phys. B* **28**, L341 (1993).

- [18] F. Maulbetsch and J.S. Briggs, *J. Phys. B* **27**, 4095 (1994).
- [19] M. Pont and R. Shakeshaft, *Phys. Rev. A* **51**, R2676 (1995).
- [20] F.W. Byron, Jr. and C.J. Joachain, *Phys. Rev.* **164**, 1 (1967).
- [21] Y.F. Smirnov, A.V. Pavlitchenkov, V.G. Levin, and V.G. Neudatchin, *J. Phys. B* **11**, 3587 (1978).
- [22] C. Dal Cappello and H. Le Rouzo, *Phys. Rev. A* **43**, 318 (1991).
- [23] It would clearly be desirable to combine models 2 and 3. While the relevant photo cross sections can again be evaluated analytically [22], the results are prohibitively complex with regards to subsequent phase-space integrations on the computers available for this project.
- [24] G.P. Lepage, *J. Comput. Phys.* **27**, 192 (1978).
- [25] Note that the presence of a signature of the second photon “pulse” in the numerical data indicates that the applicability of the equivalent-photon method to this kinematical situation has to be put in question: the analogy between this pulse and the physical electromagnetic field is not exact.
- [26] G.H. Wannier, *Phys. Rev.* **90**, 817 (1953).